Jpn. J. Appl. Phys. Vol. 41 (2002) pp. 6440–6442
Part 1, No. 11A, November 2002

Protonic Conduction in the Single Crystal of Sc-Doped $SrZrO_3$

Tohru HIGUCHI, Takeyo TSUKAMOTO, Shu YAMAGUCHI[1], Noriko SATA[2*], Kiyohisa HIRAMOTO[2†], Mareo ISHIGAME[2‡] and Shik SHIN[3,4]

Department of Applied Physics, Tokyo University of Science, Tokyo 162-8601, Japan
[1]*Department of Materials Science, University of Tokyo, Tokyo 113-8656, Japan*
[2]*Institute of Multidisciplinary Research for Advanced Materials, Research Building of Scientific Measurements, Tohoku University, Sendai 980-8577, Japan*
[3]*Institute for Solid State Physics, University of Tokyo, Chiba 277-8581, Japan*
[4]*RIKEN, Hyogo 679-5143, Japan*

(Received May 9, 2002; accepted for publication July 17, 2002)

The protonic conduction of Sc-doped $SrZrO_3$ ($SrZr_{1-x}Sc_xO_3$) in the single crystal form is investigated. The $SrZr_{1-x}Sc_xO_3$ crystals exhibit significantly higher conductivity than the pure ones, and the crystal with $x = 0.05$ exhibits the highest conductivity of those masured. The activation energy of the $SrZr_{1-x}Sc_xO_3$ crystal decreases rapidly with increasing Sc^{3+} concentration when $x \leq 0.05$, and increases when $x > 0.05$. The activation energy of $SrZr_{0.95}Sc_{0.05}O_3$ agrees with the energy separation between hole states at the top of the valence band and the Fermi level. [DOI: 10.1143/JJAP.41.6440]

KEYWORDS: protonic conductivity, $SrZr_{1-x}Sc_xO_3$, hole, activation energy, XAS

1. Introduction

Perovskite-type oxides, such as $SrCeO_3$, $SrZrO_3$ and $SrTiO_3$, exhibit hole conductivity as well as protonic conductivity in the very high temperature region when doped with acceptor ions.[1–6] These protonic conductors are important materials for a wide variety of electrochemical applications such as fuel cells and hydrogen sensors in the renewable energy source industry. Therefore, understanding the proton storage or conduction mechanism is important for further applications.

The protonic conduction of $SrZr_{1-x}M_xO_3$ doped with four acceptor ions ($M^{3+} = Y^{3+}$, Sc^{3+}, Yb^{3+}, Er^{3+}) in the single crystal form was studied.[5,7] The protonic conductivity was found in four acceptor ions, indicating that the protons migrate by hopping from site to site. From the isotope effect, it was clarified that the conductivity is referred to the hole conduction at temperatures above 700°C and to the protonic conduction below 500°C. The conductivity and the activation energy decrease with increasing the ionic radius of the acceptor, indicating that the O–H bond strength changes with ionic radius of the acceptor. The main charge carrier can be a proton, an oxygen ion or a hole, and the dominant protonic conductivity region depends on the number of oxygen vacancies or hydrogen fugacity. The number of main charge carriers also depends on the protonic conductivity. In Y^{3+}-doped $SrZrO_3$ ($SrZr_{1-x}Y_xO_3$), the protonic conductivity increases significantly with the concentration of Y^{3+} ions and becomes almost constant at $x > 0.05$.[2]

In recent years, theoretical and experimental investigations of the microscopic mechanism of proton migration have been extensively conducted in perovskite-type protonic conductors.[8–18] Matsuo *et al.* studied local proton dynamics by spectral hole burning spectroscopy.[15] In Sc^{3+}- and Y^{3+}-doped $SrZrO_3$, they reported that the values of the potential barriers for local protonic motion were several times lower than the activation energy (E_A) obtained by electrical conductivity measurements. On the other hand, the electronic structures of Sc-doped $SrTiO_3$ and In-doped $CaZrO_3$ have been studied by X-ray absorption spectroscopy (XAS). The XAS spectra show two features whose energy positions match the hole state at the top of the valence band and the proton-induced level near the Fermi level (E_F). It is reported that the energy separation agrees with E_A.[16–18] However, the detailed electrical properties and the electronic structure of acceptor-doped $SrZrO_3$ have not been clarified thus far.

In this study, the Sc^{3+} concentration dependence of the electrical conductivity of Sc-doped $SrZrO_3$ ($SrZr_{1-x}Sc_xO_3$) was measured in the temperature region from 30 to 900°C in H_2O atmosphere. Furthermore, the O 1*s* XAS spectra of proton-doped crystals were also measured. We discuss how the activation energy of the protonic conductor $SrZr_{1-x}Sc_xO_3$ is related to the electronic structure.

2. Experimental

The $SrZr_{1-x}Sc_xO_3$ samples were prepared by the solid-state reaction of $SrZrO_3$, $SrCO_3$, and Sc_2O_3 at 1200°C for about 12 h, and single crystals were grown by a floating zone method using a Xe-arc imaging furnace. The single crystals were grown in O_2 atmosphere to prevent the protons. The prepared crystals were transparent and shaped like rectangular columns of about $1.5 \times 0.8 \times 8\,mm^3$. The Sc^{3+} ion was found to be doped as an acceptor ion in the Zr^{4+} ion site of $SrZrO_3$ by a simple thermoelectromotive force experiment. The Sc^{3+} dopant concentration changed from $x = 0$ to 0.10. The single crystals were confirmed to be a single phase with perovskite structure by the powder X-ray diffraction analysis. The prepared crystals were annealed in an atmosphere of saturated H_2O vapor pressure ($P_{H_2O} = 0.03$ atm) at 20°C for 3 h in order to introduce protons into the crystal.

Complex impedance was measured by the HP4275A LCR meter from room temperature to 900°C. The experimental system was described in ref. 2. The electrical conductivity was determined from the Cole–Cole complex impedance plot at each temperature.

XAS measurements were carried out at the revolver undulator beamline BL-19B at the Photon Factory (PF) of the High Energy Accelerator Organization (KEK), Tsukuba, Japan. Synchrotron radiation from the undulator was

*Present address: Faculty of Engineering, Tohoku University, Sendai 980-8579, Japan.
†Present address: Central Research Laboratory, Hitachi Ltd., Tokyo 185-8601, Japan.
‡Present address: Akita Technical College, Akita 011-0923, Japan.

monochromatized using a grating monochromator. The revolver undulator covers a wide energy range from 10 to 1200 eV in the first harmonic.[19,20] High brightness with high resolution is realized using a varied line-spacing plane grating monochromator. A resolution of about $\Delta E/E = 2\times 10^{-4}$ at $h\nu = 400$ eV and a high photon flux of about 10^{12}–10^{13} photons/s is realized with a spot size of 100 μm.[10,11] The XAS spectra were measured by collecting the total fluorescence yield.

3. Results and Discussion

Figure 1 shows the Arrhenius plots of the electrical conductivity as a function of Sc^{3+} ion concentration in $SrZr_{1-x}Sc_xO_3$ measured in an atmosphere of saturated H_2O vapor at 20°C. For reference, the Arrhenius plot for $SrZrO_3$ ($x = 0$) is also measured and the results are shown in the figure. It is clear that the conductivity at $x = 0$ is different from that of Sc^{3+}-doped crystals. The conductivity of $SrZr_{1-x}Sc_xO_3$ exhibits thermal activation-type behavior in the temperature region of 30 to 900°C. The conductivities increase significantly with increasing Sc^{3+} dopant concentration when $x \leq 0.05$, and decrease slightly when $x > 0.05$. The Arrhenius plots are divided into two regions, namely, a high-temperature region above ~500°C, and a low-temperature region below ~500°C. Each temperature region has a different slope, which is attributed to the difference in the activation energy. From a recent report,[2,3,5] it is clarified that hole and oxygen vacancy conductions are dominant in the high-temperature region, and proton conduction is dominant in the low-temperature region. This result resembles the conductivities of Y^{3+}-, Yb^{3+}-, and Er^{3+}-doped $SrZrO_3$ crystals.

Figure 2(a) shows the electrical conductivity measured at about 100°C shown in Fig. 1 vs Sc^{3+} dopant concentration (mol%). The conductivity increases significantly with increasing Sc^{3+} dopant concentration when $x \leq 0.05$, but decreases slightly when $x > 0.05$. Sc^{3+} ions produce holes and protons, leading to the increase of the conductivity when $x \leq 0.05$; however, highly doped crystals structures are slightly distorted, leading to the decrease of the conductivity when $x > 0.05$. The crystal with $x = 0.05$ exhibits the highest conductivity. Furthermore, the activation energy (E_A) estimated from the slope of the Arrhenius plot is shown

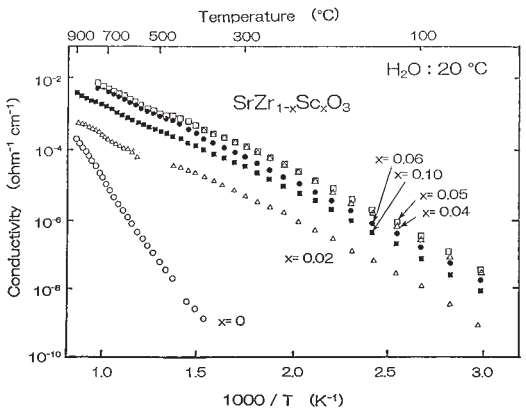

Fig. 1. Arrhenius plot of the electrical conductivity as a function of Sc^{3+} doping of proton-doped $SrZr_{1-x}Sc_xO_3$ measured in an atmosphere of saturated H_2O vapor at 20°C.

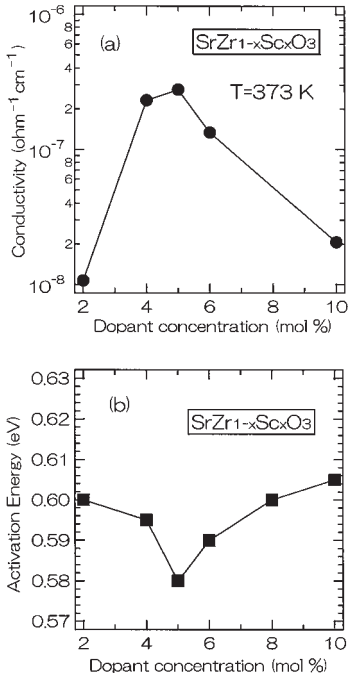

Fig. 2. (a) Electrical conductivity at about 100°C and (b) E_A estimated from the slope of the Arrhenius plot vs Sc^{3+} dopant concentration.

in Fig. 2(b). The E_A decreases significantly from 0.60 to 0.58 eV when $x \leq 0.05$ and increases from 0.58 to 0.61 eV when $x > 0.05$. The crystal with $x = 0.05$ exhibits the minimum E_A. This behavior resembles the result of Sc-doped $SrTiO_3$.[6] The above results indicate that proton or hole conduction depends on the Sc^{3+} dopant concentration.

Figure 3 shows the O 1*s* XAS spectra of proton-doped $SrZrO_3$ and $SrZr_{0.95}Sc_{0.05}O_3$. From the dipole selection rule, it is understood that the O 1*s* XAS spectra of Zr oxides

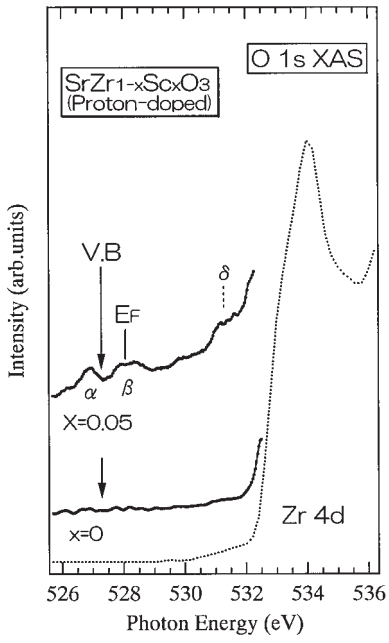

Fig. 3. Comparison of the O 1*s* XAS spectra of proton-doped $SrZrO_3$ and $SrZr_{0.95}Sc_{0.05}O_3$. Thick lines show the O 1*s* XAS spectra on a magnified scale. Vertical bar represents the position of the E_F determined from the binding energy of the O 1*s* photoemission peak. Arrows indicate the top of the valence band.

correspond to transition from O 1*s* character to O 2*p* character hybridized with unoccupied Zr 4*d* states.[18,21,22] The O 1*s* XAS spectra are normalized by the Sr 4*d* peak of the conduction band, although the peak is not shown in this figure. The feature around ~534 eV is mainly composed of the Zr 4*d* state hybridized with the O 2*p* state. The spectral intensity below the threshold is magnified ten times and is shown as a thick line above each XAS spectrum in order to obtain reliable information in the band gap energy region. In this energy region, the electronic structure related to the proton conductivity can be elucidated. Arrows show the top of the valence band. The Fermi level (E_F) is determined from the binding energy of the O 1*s* photoemission peak.

It is striking that the three features corresponding to α, β and δ peaks are observed in the band gap energy region of proton-doped $SrZr_{0.95}Sc_{0.05}O_3$, although there is no structure in the band gap of nondoped $SrZrO_3$. The weak feature δ is considered to be a defect-induced level of the Zr 4*d* state, since the feature is located at the bottom of the Zr 4*d* conduction band. The feature α may be assigned to holes created by Sc^{3+} doping at the top of the valence band, which is mainly composed of nonbonding O 2*p* states in the valence band. In the absorption spectra in the vacuum ultraviolet region, it has been reported that the band gap of $SrZr_{1-x}Y_xO_3$ increases with increasing Y^{3+} ion concentration,[13] indicating the presence of holes created at the top of the valence band. Such a situation is also expected in $SrZr_{1-x}Sc_xO_3$. Furthermore, the feature β at or near E_F splits into two structures, which may be assigned to the acceptor- and proton-induced levels, as expected from the rigid-band model. The energy separation between the hole state and E_F is about 0.6 eV. This value is near the activation energy estimated from the electrical conductivity and the potential barrier for proton hopping in hydrogen bonding systems calculated by Isram,[12] indicating the hopping conduction between the hole state at the top of the valence band and the acceptor or proton-induced level.

4. Conclusions

We studied the protonic conduction in the single crystal of $SrZr_{1-x}Sc_xO_3$. The electrical conductivity is related to the hole conduction at temperatures above 500°C and to the proton conduction below 500°C. The doped crystals exhibit sufficiently higher conductivities than the pure ones, and the crystal with $x = 0.05$ exhibits the highest conductivity of those measured. E_A decreases rapidly with increasing Sc^{3+} concentration when $x \leq 0.05$, and increases when $x > 0.05$. In the O 1*s* XAS spectra, the hole state and acceptor- or proton-induced level were observed at the top of the valence band and E_F, respectively. The energy separation between the hole state and E_F agrees with E_A obtained by electrical conductivity measurements.

Acknowledgements

This work was partly supported by the Foundation for Material Science and Technology of Japan (MST Foundation) and a Grant-in-Aid for Science Research (No. 13740191) from the Ministry of Education, Culture, Sports, Science and Technology.

1) H. Iwahara, T. Esaka, H. Uchida and N. Maeda: Solid State Ionics **3–4** (1980) 359.
2) S. Shin, H. H. Huang, M. Ishigame and H. Iwahara: Solid State Ionics **47** (1990) 910.
3) H. H. Huang, M. Ishigame and S. Shin: Solid State Ionics **47** (1991) 251.
4) N. Sata, K. Hiramoto, M. Ishigame, S. Hosoya, N. Niimura and S. Shin: Phys. Rev. B **54** (1996) 15795.
5) T. Higuchi, T. Tsukamoto, N. Sata, K. Hiramoto, M. Ishigame and S. Shin: Jpn. J. Appl. Phys. **40** (2001) 4162.
6) T. Higuchi, T. Tsukamoto, K. Hiramoto, M. Ishigame and S. Shin: Jpn. J. Appl. Phys. **41** (2002) 2120.
7) H. Yugami, Y. Shibayama, S. Matsuo, M. Ishigame and S. Shin: Solid State Ionics **85** (1996) 319.
8) F. Shimojo, K. Hoshino and H. Okazaki: J. Phys. Soc. Jpn. **65** (1996) 1143.
9) F. Shimojo, K. Hoshino and H. Okazaki: J. Phys. Soc. Jpn. **66** (1997) 8.
10) F. Shimojo, K. Hoshino and H. Okazaki: J. Phys. Soc. Jpn. **67** (1998) 2008.
11) Z.-Q. Li, J.-L. Zhu, C. Q. Wu, Z. Tang and Y. Kawazoe: Phys. Rev. B **58** (1998) 8075.
12) M. S. Isram: J. Mater. Chem. **10** (2000) 1027.
13) N. Sata, M. Ishigame and S. Shin: Solid State Ionics **86–88** (1996) 629.
14) N. Sata, S. Shin, K. Shibata and M. Ishigame: J. Phys. Soc. Jpn. **68** (1999) 3600.
15) S. Matsuo, H. Yugami and M. Ishigame: Phys. Rev. B **64** (2001) 24302.
16) T. Higuchi, T. Tsukamoto, K. Kobayashi, S. Yamaguchi, N. Sata, M. Ishigame, Y. Ishiwata and S. Shin: Solid State Ionics **136–137** (2000) 261.
17) T. Higuchi, T. Tsukamoto, Y. Tezuka, K. Kobayashi, S. Yamaguchi and S. Shin: Jpn. J. Appl. Phys. **39** (2000) L 133.
18) S. Yamaguchi, K. Kobayashi, T. Higuchi, S. Shin and Y. Iguchi: Solid State Ionics **136–137** (2000) 305.
19) S. Shin, A. Agui, M. Fujisawa, Y. Tezuka, T. Ishii and N. Hirai: Rev. Sci. Instrum. **66** (1995) 1584.
20) M. Fujisawa, A. Harasawa, A. Agui, M. Watnabe, A. Kakizaki, S. Shin, T. Ishii, T. Kita, T. Harada, Y. Saitoh and S. Suga: Rev. Sci. Instrum. **67** (1996) 345.
21) T. Higuchi, T. Tsukamoto, K. Kobayashi, Y. Ishiwata, M. Fujisawa, T. Yokoya, S. Yamaguchi and S. Shin: Phys. Rev. B **61** (2000) 12860.
22) T. Higuchi, T. Tsukamoto, K. Kobayashi, Y. Ishiwata, T. Yokoya, S. Yamaguchi and S. Shin: Phys. Rev. B **65** (2002) 033201.